Radek Fučík; Jiří Mikyška
Numerical investigation of dynamic capillary pressure in two-phase flow in porous medium

NUMERICAL INVESTIGATION OF DYNAMIC CAPILLARY PRESSURE IN TWO-PHASE FLOW IN POROUS MEDIUM

Radek Fučík, Jiří Mikyška, Praha

Abstract. In order to investigate effects of the dynamic capillary pressure-saturation relationship used in the modelling of a flow in porous media, a one-dimensional fully implicit numerical scheme is proposed. The numerical scheme is used to simulate an experimental procedure using a measured dataset for the sand and fluid properties. Results of simulations using different models for the dynamic effect term in capillary pressure-saturation relationship are presented and discussed.

Keywords: dynamic capillary pressure, two-phase flow in porous media, immiscible displacement in porous media, finite volume method

MSC 2010: 65N06, 35K55

1. Introduction

In the description of the behavior of immiscible and incompressible fluids within porous media, a rigorous definition and a reliable model of the capillarity are crucial. In the past decades, various capillary pressure-saturation models were correlated from laboratory experiments under equilibrium conditions. These *static* capillary pressure models such as [3] or [15] have been used in most of the mathematical studies on modelling of a multiphase flow in a porous medium. However, it was found that the laboratory measured capillary pressure does not correspond to the capillary pressure in the case of large velocities. As a result of the empirical approach in [14], new two-phase flow theories were developed in [6], [7], or [8]. The most important result is that the static capillary pressure-saturation relationship cannot be used in the modelling of capillarity when the fluid content is in motion and, therefore, a new model of the capillary pressure-saturation relationship is proposed and referred to as the dynamic capillary pressure.

The two-phase flow system can be simplified to the Richards problem, in which the pressure of the non-wetting phase (air or oil) is assumed to be constant. This is the case in [11] where the dynamic effects are not found to be relevant for the given structure of heterogeneous porous medium. The relevance of using the dynamic capillary pressure in the full two-phase flow system of equations has not been fully answered yet. For instance, in [10], the authors present a semi-implicit numerical scheme based on the first-order upwind finite volume method where the material interfaces are treated by Lagrange multipliers. However, in that paper, only the constant dynamic effect coefficient was considered whereas other researchers suggest more general functional models for the dynamic effect coefficient as in [13].

A fully implicit numerical scheme is proposed that can be used for a detailed investigation of the saturation and capillary pressure behavior when the dynamic capillary pressure is used instead of the static capillary pressure in the full two-phase flow system. The aim is to investigate the behavior of different functional models of the dynamic capillary pressure coefficient. Moreover, the material interface condition for the dynamic capillary pressure is treated in a new, modified way based on the standard extended capillary pressure condition as in [9].

2. Mathematical model

We present the mathematical model describing the two-phase flow in a one-dimensional porous medium in this section. Two phases—a wetting phase (indexed w) and a non-wetting phase (indexed n)—are considered to be present within the pores of the porous medium and both fluids are assumed to be incompressible and immiscible. Under these assumptions, the one-dimensional $p_w - S_n$ formulation in a domain $\Omega = [0, L]$ is given by

$$(2.1) \qquad \Phi\frac{\partial S_\alpha}{\partial t} + \frac{\partial u_\alpha}{\partial x} = 0,$$

$$(2.2) \qquad u_\alpha = -\frac{k_{r\alpha}}{\mu_\alpha}K\Big(\frac{\partial}{\partial x}(p_w + \delta_{\alpha n}p_c) - \varrho_\alpha g\Big),$$

where $S_w + S_n = 1$, $\delta_{\alpha n}$ is the Kronecker symbol, and $\alpha \in \{w, n\}$. S_α denotes the saturation, p_α is the pressure, ϱ_α is the volumetric density, μ_α is the dynamic viscosity, $k_{r\alpha}$ is the relative permeability of the phase α, where $\alpha \in \{w, n\}$. The Darcy velocities are denoted by u_α. Symbols Φ, K, and g stand for porosity, permeability of the soil matrix and gravitational acceleration, respectively.

Governing equations (2.1) and (2.2) are subject to an initial condition

$$(2.3) \qquad S_\alpha = S_\alpha^0, \quad \text{in } \Omega,$$

and boundary conditions

$$(2.4) \qquad u_\alpha \cdot n = u_\alpha^N, \quad \text{on } \Gamma_{u_\alpha}^N,$$

$$(2.5) \qquad S_\alpha = S_\alpha^D, \quad \text{on } \Gamma_S^D,$$

$$(2.6) \qquad p_\alpha = p_\alpha^D, \quad \text{on } \Gamma_{p_\alpha}^D,$$

where n denotes the outer normal vector to the boundary. Generally, $\Gamma_{u_\alpha}^N$, Γ_S^D, and $\Gamma_{p_\alpha}^D$ denote subsets of the boundary Γ of the domain Ω, here, $\Gamma = \{0, L\}$.

Following the standard definitions in literature, the capillary pressure p_c on the pore scale is defined as the difference between the non-wetting phase pressure p_n and the wetting phase pressure p_w, i.e.,

$$(2.7) \qquad p_c = p_n - p_w.$$

On the macroscale, the capillary pressure has been commonly considered to be a function of the wetting phase saturation only [9], [1], [2]. The following Brooks and Corey [3] capillary pressure-effective wetting phase saturation parametrization is used in the presented two-phase flow model:[1]

$$(2.8) \qquad p_c^{eq} = p_d (S_w^e)^{-1/\lambda},$$

where p_d is the entry pressure, λ is the pore size distribution index, and S_w^e is the effective saturation of the wetting phase defined as

$$(2.9) \qquad S_\alpha^e = \frac{S_\alpha - S_{r\alpha}}{1 - \sum_\beta S_{r\beta}},$$

where $S_{r\alpha}$ is the α-phase irreducible saturation.

The Brooks and Corey relationship (2.8) is suitable for modelling a flow in heterogeneous porous media because the difference in the entry pressure coefficients p_d in different porous materials captures the barrier effect that has been observed in various experiments [12], [9]. Together with the Brooks and Corey model of p_c given by (2.8), the Burdine model for the relative permeability functions $k_{r\alpha}$ reads

$$(2.10) \qquad k_{rw} = (S_w^e)^{3+2/\lambda}, \quad k_{rn} = (1 - S_w^e)^2 (1 - (S_w^e)^{1+2/\lambda}).$$

The dynamic capillary pressure-saturation relationship is proposed in the form [7]

$$(2.11) \qquad p_c := p_n - p_w = p_c^{eq} - \tau \frac{\partial S_w}{\partial t},$$

---

[1] A superscript ^{eq} is used in the definition (2.8) with respect to the following text and it indicates the model of the capillary pressure for the system in the state of thermodynamic equilibrium.

where p_c^{eq} is the capillary pressure-saturation relationship in the thermodynamic equilibrium of the system and τ, the dynamic effect coefficient, is a material property of the system.

In this paper, we consider a general nonlinear dependence $\tau = \tau(S_w)$ based on a laboratory measured dataset. In particular, we will use constant, linear, and log-linear functional models of $\tau = \tau(S_w)$ correlated from the dataset. The laboratory experiment is described briefly in Section 4.

3. Numerical model

We propose a standard finite volume discretization technique in order to determine approximate discrete solutions $S_{n,i}^k$ and $p_{w,i}^k$ of the problem (2.1), generally denoted by $f_i^k = f(k\Delta t, i\Delta x)$, where $i = 0, 1, \ldots, m$, $m\Delta x = L$, $k = 0, 1, \ldots, n$, and $n\Delta t = T$. The length of the domain is denoted by L and the final time of the simulation by T.

The fully implicit numerical scheme reads

$$(3.1) \qquad \Phi \frac{S_{\alpha,i}^{k+1} - S_{\alpha,i}^k}{\Delta t} = -\frac{u_{\alpha,i+1/2}^{k+1} - u_{\alpha,i-1/2}^{k+1}}{\Delta x},$$

where $\alpha \in \{w, n\}$. The discrete Darcy velocities u_α introduced by (2.2) are given by

$$(3.2) \qquad u_{\alpha,i+1/2}^{k+1} = -\frac{K}{\mu_\alpha} k_{r\alpha}(S_{\alpha,upw}^{k+1}) \Big(\underbrace{\frac{p_{w,i+1}^{k+1} - p_{w,i}^{k+1}}{\Delta x} + \delta_{\alpha n} \frac{p_{c,i+1}^{k+1} - p_{c,i}^{k+1}}{\Delta x} - \varrho_\alpha g}_{\Delta\Phi_\alpha} \Big),$$

and the discrete capillary pressure by

$$(3.3) \qquad p_{c,i}^{k+1} = p_c \Big(1 - S_{n,i}^{k+1}, -\frac{S_{n,i}^{k+1} - S_{n,i}^k}{\Delta t} \Big)$$

$$= p_c^{eq}(1 - S_{n,i}^{k+1}) + \tau(1 - S_{n,i}^{k+1}) \frac{S_{n,i}^{k+1} - S_{n,i}^k}{\Delta t},$$

where $S_{\alpha,upw}^{k+1}$ is the saturation taken in the upstream direction with respect to the gradient of the phase potential Φ_α, i.e.

$$S_{\alpha,upw}^{k+1} = \begin{cases} S_{\alpha,i+1}^{k+1} & \text{if } \Delta\Phi_\alpha \geqslant 0, \\ S_{\alpha,i}^{k+1} & \text{if } \Delta\Phi_\alpha < 0. \end{cases}$$

The fully implicit numerical scheme is solved using the Newton-Raphson iteration method. The Jacobi matrix is block tridiagonal and therefore solved by the Thomas
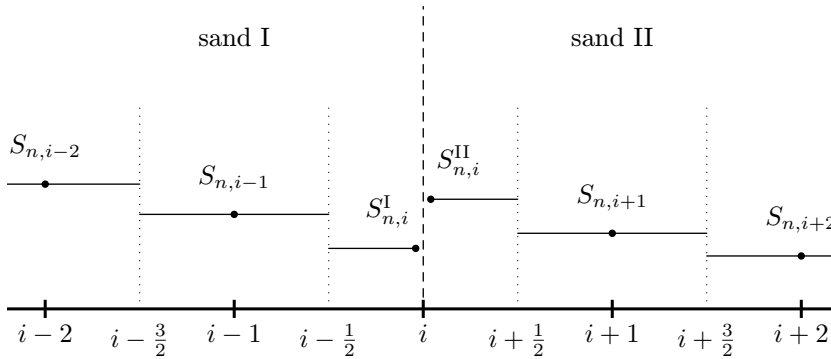
Figure 1. Discretization of the saturation jump at material discontinuity.

algorithm. In each iteration, a new guess of discrete saturation $S_{n,i}^{k+1}$ is given (in the current time step $k+1$) and the upstream saturations in (3.2) are recomputed. In practice, less than 25 iterations are needed to achieve a sufficient precision about 10^{-7} using the L_2-norm. In the numerical simulation, Δt is chosen using the adaptive strategy based on the iteration limit chosen. If the number of iterations exceeds some threshold value, the time step Δt is lowered and the Newton-Raphson iteration method is restarted. Otherwise, we increase Δt regularly.

In general, we need to choose Δt and Δx small enough in order to achieve sufficient convergence. This can be shown by comparing the numerical solution to the semi-analytical solutions derived by our group in [4] and [5] that are available when several restrictions are placed upon the problem formulation (2.1). The stability of the numerical scheme presented can be investigated by means of the Fourier analysis in the case of the numerical scheme (3.1) applied to a simplified version of the nonlinear problem equations (2.1) and (2.2) written in the form of a single Sobolev differential equation with constant coefficients

$$(3.4) \qquad \frac{\partial S_w}{\partial t} + A\frac{\partial S_w}{\partial x} = D\frac{\partial^2 S_w}{\partial x^2} + T\frac{\partial^3 S_w}{\partial x^2 \partial t}.$$

It can be shown that the numerical scheme (3.1) is unconditionally stable in the case of (3.4). Analysis of the nonlinear problem (2.1) is in preparation by the authors.

4. NUMERICAL EXPERIMENTS

In this section, we use the numerical scheme (3.1) to simulate the laboratory experiment that was carried out in the Center for Experimental Study of Subsurface Environmental Processes, Colorado School of Mines. As a result of this experiment, three functional models of the dynamic effect coefficient $\tau = \tau(S_w)$ were correlated.

Models of the dynamic effect coefficient $\tau = \tau(S_w)$ were estimated as a result of the laboratory experiment, which consisted of a single, vertically placed, 10 cm long tube uniformly filled with a homogeneous sand. Initially, the column is flushed with water such that no air phase is present inside. A series of slow drainage steps was carried out in order to determine the capillary pressure-saturation relationship in equilibrium p_c^{eq}. The measured Brooks and Corey model parameters are shown in Table 2. Then, a series of fast drainage and imbibition experiments was performed and the values of the capillary pressure and the air saturation are measured by probes in the middle of the column. Based on these measurements, three models of the dynamic effect coefficient τ were correlated (see Table 3).

We simulate the experiment as a one-dimensional problem with different models of $\tau(S_w)$. The parameters of the discrete problem (3.1) are summarized in Table 1. The resulting temporal profiles of the air saturation S_n and the capillary pressure p_c are shown in Figure 2. In these numerical simulations, the measured outflow of water is used as a Neumann boundary condition at the bottom of the column ($x = L$).
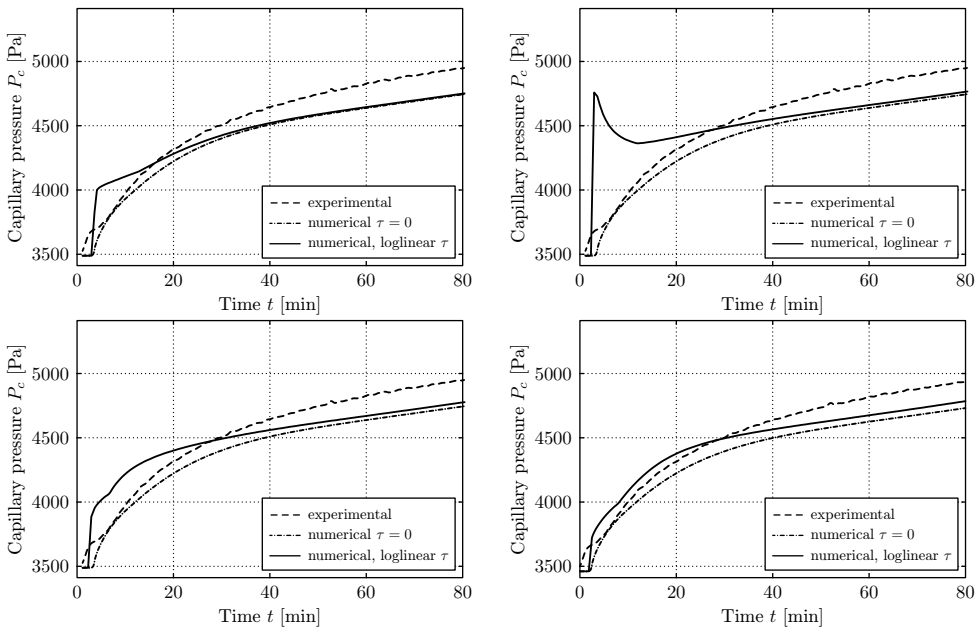

Figure 2. Numerical solutions with smooth boundary flux and laboratory measured S_n and p_c in the middle of the column for various models of $\tau = \tau(S_w)$. Numerical solutions were obtained with $m = 1600$ nodes.

The influence of different models of the dynamic effect coefficient τ on the numerical solution of the air saturation S_n is found to be negligible. On the other hand, their influence on the capillary pressure p_c is important in the cases where there

Initial condition	$S_n(x,0) = 0$	$\forall x \in (0, L)$
Boundary conditions	$u_n(0, t) = 0$	$\forall t \in [0, T]$
	$p_n(0, t) = \text{const} = 0$	$\forall t \in [0, T]$
	$u_w(L, t) = 3.7 \cdot 10^{-5} \exp(-1.7 \cdot 10^{-3} t)$	
	$\qquad + 7.4 \cdot 10^{-7} \; [\text{ms}^{-1}].$	$\forall t \in [0, T]$
	$u_n(L, t) = 0$	$\forall t \in [0, T]$
Problem setup	$T = 5000\,\text{s},\ L = 10\,\text{cm},\ g = 9.81\,\text{ms}^{-2}$	
Capillary pressure	Dynamic capillary pressure p_c,	
	various models for $\tau(S_w)$, see Table 3	
Sand	Ohji sand, Table 2	
Fluids	Air and water, Table 4	

Table 1. Parameters of the simulation of the laboratory experiment

Parameter			Ohji sand
Porosity	Φ	[−]	0.448
Intrinsic permeability	K	[m^2]	$1.63 \cdot 10^{-11}$
Residual water saturation	S_{wr}	[–]	0.265
Brooks-Corey entry pressure	p_d	[Pa]	3450
Brooks-Corey pore size dist. index	λ	[–]	4.66

Table 2. Properties of porous media used in the numerical simulation.

Model of τ [Pa s]	Ohji sand
Stauffer model	$\tau(S_w) = \tau_{\text{S,Ohji}} = 3.3 \cdot 10^5$
Constant model	$\tau_{Ohji}(S_w) = 1.1 \cdot 10^6$
Linear model	$\tau_{Ohji}(S_w) = 3.2 \cdot 10^6 (1 - S_w)$
Loglinear model	$\tau_{Ohji}(S_w) = 10^8 \exp(-7.7 S_w)$

Table 3. Experimentally determined models of the dynamic effect coefficient τ for the Ohji sand.

Parameter			Water	Air
Density	ϱ	[kgm^{-3}]	997.8	1.205
Dyn. viscosity	μ	[kgm^{-1}s^{-1}]	$9.77 \cdot 10^{-4}$	$1.82 \cdot 10^{-5}$

Table 4. Fluid properties used in the simulations.

is a temporal change in the saturation S_n because the temporal derivative of S_n is multiplied by the dynamic effect coefficient τ in (2.11). The constant model for τ does not seem to be a good model for the appropriate approximation because its numerical solution of p_c differs substantially from the measured capillary pressure (see Figure 2). Therefore, the constant model requires further investigation of its validity.

5. Conclusions

A one-dimensional numerical scheme of two-phase incompressible and immiscible flow is presented that enables simulation of two-phase flow in homogeneous porous media under dynamic capillary pressure conditions.

Laboratory measured parameters were used in the numerical simulation of the dynamic capillary pressure including three models of the dynamic effect coefficient $\tau = \tau(S_w)$. The numerical solutions for the non-static capillary pressure show that the dynamic effect has a significant impact on the magnitude of the capillary pressure while the change in the saturation profiles may be considered negligible in some cases. The constant model of τ showed rather unrealistic profile of the numerical approximation of the capillary pressure when compared to the laboratory measured data.

Results of the simulation indicate that the dynamic effect may not be so important in drainage problems in a homogeneous porous medium. However, it may be of great importance in highly heterogeneous media where the capillarity governs flow through material interfaces.

References

[1] *P. Bastian*: Numerical Computation of Multiphase Flows in Porous Media. Habilitation Dissertation, Kiel University, 1999.

[2] *J. Bear, A. Verruijt*: Modeling Groundwater Flow and Pollution. D. Reidel, Dordrecht, 1990.

[3] *R. H. Brooks, A. T. Corey*: Hydraulic properties of porous media. Hydrology Paper *3* (1964).

[4] *R. Fučík, J. Mikyška, M. Beneš, T. H. Illangasekare*: An improved semi-analytical solution for verification of numerical models of two-phase flow in porous media. Vadose Zone Journal *6* (2007), 93–104.

[5] *R. Fučík, J. Mikyška, M. Beneš, T. H. Illangasekare*: Semianalytical solution for two-phase flow in porous media with a discontinuity. Vadose Zone Journal *7* (2008), 1001–1007.

[6] *W. G. Gray, S. M. Hassanizadeh*: Paradoxes and realities in unsaturated flow theory. Water Resources Research *27* (1991), 1847–1854.

[7] *W. G. Gray, S. M. Hassanizadeh*: Unsaturated flow theory including interfacial phenomena. Water Resources Research *27* (1991), 1855–1863.

[8] *S. M. Hassanizadeh, W. G. Gray*: Thermodynamic basis of capillary pressure in porous media. Water Resources Research *29* (1993), 3389–3406.

[9] *R. Helmig*: Multiphase Flow and Transport Processes in the Subsurface: A Contribution to the Modeling of Hydrosystems. Springer, Berlin, 1997.

[10] *R. Helmig, A. Weiss, B. I. Wohlmuth*: Dynamic capillary effects in heterogeneous porous media. Comput. Geosci. *11* (2007), 261–274.

[11] *O. Ippisch, H.-J. Vogel, P. Bastian*: Validity limits for the van Genuchten-Mualem model and implications for parameter estimation and numerical simulation. Advances in Water Resources *29* (2006), 1780–1789.

[12] *J. Mikyška, M. Beneš, T. H. Illangasekare*: Numerical investigation of non-aqueous phase liquid behavior at heterogeneous sand layers using voda multiphase flow code. Journal of Porous Media *12* (2009), 685–694.

[13] *T. Sakaki, D. M. O'Carroll, T. H. Illangasekare*: Direct Laboratory Quantification of Dynamic Coefficient of a Field Soil for Drainage and Wetting Cycles. American Geophysical Union, Fall Meeting 2007, abstract# H53F-1486, 2007.

[14] *F. Stauffer*: Time dependence of the relations between capillary pressure, water content and conductivity during drainage of porous media. On Scale Effects in Porous Media, IAHR, Thessaloniki, Greece, 1978.

[15] *M. T. van Genuchten*: A closed-form equation for predicting the hydraulic conductivity of unsaturated soils. Soil Science Society of America Journal *44* (1980), 892–898.

Author's address: *Radek Fučík, Jiří Mikyška* Department of Mathematics, Faculty of Nuclear Sciences and Physical Engineering, Czech Technical University, Praha, e-mail: `radek.fucik@fjfi.cvut.cz`.